Physica E 43 (2011) 1813–1819

Contents lists available at ScienceDirect

Physica E

journal homepage: www.elsevier.com/locate/physe

Nonlinear vibration of a double-walled carbon nanotube embedded in a polymer matrix

M.H. Mahdavi, L.Y. Jiang*, X. Sun

Department of Mechanical and Materials Engineering, The University of Western Ontario, London, Ontario, Canada N6A 5B9

ARTICLE INFO

Article history:
Received 26 April 2011
Received in revised form
13 June 2011
Accepted 16 June 2011
Available online 28 June 2011

Keywords:
Nonlinear interaction
Polymer composite
Timoshenko beam model
Nonlinear vibration
Harmonic balance method

ABSTRACT

In the current work, the nonlinear vibration of an embedded double-walled carbon nanotube (DWCNT) aroused by nonlinear van der Waals (vdW) interaction forces from both surrounding medium and adjacent tubes is studied. Using both Euler–Bernoulli and Timoshenko beam models, the relation between deflection amplitudes and resonant frequencies of the DWCNT is derived through harmonic balance method. It is found that the nonlinear vdW forces from the surrounding medium result in noncoaxial vibration of the embedded DWCNT. The noncoaxial vibration includes both uni-directional and bi-directional vibration modes. It is found that the surrounding matrix has more prominent effect on the uni-directional vibration in comparison to the bi-directional vibration. The axial load effect on the vibrational behavior of the embedded DWCNT is also discussed. Due to the influence of the surrounding polymer, the prediction on the resonant frequencies of embedded CNTs is quite different from that for free-standing CNTs. A softening behavior for the deflection amplitude-resonant frequency relation is observed for the first time in the bi-directional vibration of the embedded DWCNT, which can only be obtained using the Timoshenko beam theory.

1. Introduction

Since the discovery of carbon nanotubes (CNTs) by Iijima [1], these novel materials have attracted tremendous attention from research communities. CNTs are found to possess superior mechanical, electrical and thermal properties [2–7], which makes them as promising candidates in the applications of nanocomposites, nanoelectronics and nanodevices [8–15]. To make the full potential applications of CNTs, understanding their mechanical behavior is essential and has become a hot topic. In particular, considerable efforts have been devoted to understand the vibrational behavior of CNTs recently [16–20].

During the past decade, several methods have been pursued to investigate and characterize the mechanical behavior of CNTs. Since controlled experiments are difficult for nanoscale materials and atomic studies are computationally expensive, many researchers have resorted to continuum mechanics models to study the mechanical behavior of CNTs. For example, elastic beam models [16–23] and elastic shell models [24–26] have been effectively used to predict resonant frequencies of CNTs. These studies, among others, have demonstrated the powerfulness of continuum mechanics, i.e., using simple formula offered by these continuum models, key parameters that affect the mechanical behavior of CNTs can be easily discovered to predict new physical phenomena. Most existing studies in literature are linear analysis on the vibrations of CNTs. However, there are much fewer studies on the nonlinear mechanical behavior of CNTs. Until recently, different aspects of nonlinearities have been explored by researchers. Considering the geometric nonlinearity caused by large transverse displacement, Yan et al. [26] predicted the nonlinear vibration behavior of a DWCNT based on the Donnell's cylindrical shell model. A similar problem was analyzed by Ke et al. [23] using nonlocal Timoshenko beam theory. For an embedded MWCNT within a polymer matrix, the surrounding medium effect on the nonlinear vibration of the CNT aroused by the geometric nonlinearity has been studied using a multiple beam model [16]. It was found that the nonlinear free vibration of the embedded CNT was significantly affected by the surrounding medium. In these studies, the interaction pressure between two adjacent tubes of the MWCNT governed by the van der Waals (vdW) was assumed to depend linearly on the difference of the radial deflections. For embedded CNTs, the surrounding medium effect was described by the Winkler model originally developed for a fiber composite [27], in which the surrounding medium was assumed to act as linear springs and the pressure exerted on the outer tube is linearly proportional to the deflection of the outermost tube.

It should be mentioned that in the absence of covalent chemical bonds and mechanical interlocking, the interaction between the CNT and the surrounding medium at interface is governed by the

* Corresponding author. Tel.: +1 519 661 2111x80422; fax: +1 519 661 3020.
E-mail address: lyjiang@eng.uwo.ca (L.Y. Jiang).

1386-9477/$ - see front matter © 2011 Elsevier B.V. All rights reserved.
doi:10.1016/j.physe.2011.06.017

vdW force. This vdW force estimated by the Lennard-Jones potential is intrinsically nonlinear [28], as well as the vdW interaction between adjacent tubes of MWCNTs [29]. Therefore, it is natural to believe that the nonlinearity of vdW forces might play an important role in the vibrational behavior of MWCNTs. The nonlinear vibration of a double-walled carbon nanotube (DWCNT) aroused by the nonlinear interlayer vdW forces between adjacent tubes was studied by Xu et al. [21]. The deflection amplitude was revealed to depend on the nonlinear factor of the vdW forces, which was found to have little effect on the coaxial free vibration but a great effect on the noncoaxial free vibration. The effect of nonlinear interfacial vdW forces from surrounding medium on the vibrational behavior of a single-walled carbon nanotube (SWCNT) embedded in a polymer matrix was studied by Mahdavi et al. [20] using both the Euler–Bernoulli and Timoshenko beam theories. It was found that the nonlinear vdW forces from the surrounding medium have significant effect on the resonant frequencies of the embedded SWCNT. These existing studies clearly indicate the significance of considering the nonlinearity of vdW forces in the study of the vibrational behavior of CNTs.

However, it appears that the influence of these nonlinear vdW forces on the dynamic property of embedded MWCNTs have not been investigated thus far. Hence, the objective of the current work is to study the nonlinear vibrational behavior of an embedded DWCNT by considering the nonlinear vdW interactions between the outer tube and the surrounding medium, and between adjacent tubes as well. Using the Euler–Bernoulli and Timoshenko beam models, the relation between the deflection amplitude and the resonant frequency will be derived. The effects of axial load and the CNT size on the nonlinear vibration of the embedded DWCNT will also be examined. The results indicate that these nonlinear vdW interaction forces existing in the embedded DWCNT have a substantial effect on its vibrational behavior.

2. Formulation of the problem

The resonant frequencies of the embedded DWCNT will be firstly studied by the Euler–Bernoulli beam model, which is easy to employ and can give a reliable prediction on the mechanical behavior of CNTs under some circumstances. Since rotary inertia and shear deformation have significant effect on the frequency analysis either at ultrahigh frequencies or for CNTs with low length-to-diameter aspect ratio [19], the Timoshenko beam model is also utilized for comparison. Based on the interfacial cohesive law [28], the nonlinear resultant pressure exerted by the surrounding medium to the embedded CNT has been derived in our previous work [20], i.e., the interfacial force per unit area exerted on the outer layer of the DWCNT is expressed in terms of the interfacial cohesive energy Φ

$$P_{\mathrm{IF}}(\delta)=\frac{\partial \Phi}{\partial \delta} \tag{1}$$

in which Φ is expressed in terms of the interfacial spacing δ as

$$\Phi(\delta)=K_{\mathrm{IF}}\left[\frac{2}{15}\left(\frac{\delta_0}{\delta}\right)^9-\left(\frac{\delta_0}{\delta}\right)^3\right] \tag{2}$$

where K_{IF} is calculated as 0.101 874 J/m^2 and $\delta_0=0.3825$ nm if the surrounding polymer matrix is taken as polyethylene for example. The equilibrium interfacial spacing δ_e can be determined by $P_{\mathrm{IF}}(\delta=\delta_e)=0$ as

$$\delta_e=\left(\frac{2}{5}\right)^{1/6}\delta_0 \tag{3}$$

As argued by Ru [30], the resultant interaction pressure exerted on the CNT defined per unit length should be proportional to the circumferential dimension, i.e., the outer radius R_2 of the DWCNT. Thus one can assume that the resultant interaction pressure per unit axial length between the CNT and the surrounding polymer matrix can be assumed as $p_{\mathrm{IF}}=-2R_2P_{\mathrm{IF}}(\delta_e)$. The Taylor expansion of p_{IF} at δ_e can be expanded up to the lowest-order nonlinear term as [20]

$$\begin{aligned} p_{IF}&=-2R_2P_{\mathrm{IF}}\big|_{\delta=\delta_e}-2R_2\frac{\partial P_{IF}}{\partial \delta}\bigg|_{\delta=\delta_e}(\delta-\delta_e)-2R_2\frac{1}{6}\frac{\partial^3 P_{IF}}{\partial \delta^3}\bigg|_{\delta=\delta_e}(\delta-\delta_e)^3\\ &=-\alpha_1w_2-\alpha_3w_2^3 \end{aligned} \tag{4}$$

where $P_{\mathrm{IF}}\big|_{\delta=\delta e}=0$ and

$$\alpha_1=2R_2\frac{\partial P_{\mathrm{IF}}}{\partial \delta}\bigg|_{\delta=\delta_e},\quad \alpha_3=2R_2\frac{1}{6}\frac{\partial^3 P_{\mathrm{IF}}}{\partial \delta^3}\bigg|_{\delta=\delta_e} \tag{5}$$

are the equivalent linear and nonlinear stiffness of the surrounding medium. The interfacial spacing change equals to the deflection w_2 of the outer layer of the DWCNT, i.e., $\delta-\delta_e=w_2$.

Similarly, the resultant interaction pressure per unit axial length between adjacent tubes of the DWCNT due to the vdW forces can be expressed in terms of the deflection w_1 and w_2 of the inner and outer tubes from the interlayer cohesive energy U [21], i.e.,

$$p_{\mathrm{IL}}=-c_1(w_2-w_1)-c_3(w_2-w_1)^3 \tag{6}$$

in which

$$c_1=2R_1\frac{\partial^2 U}{\partial \Delta^2}\bigg|_{\Delta=\Delta_e},\quad c_3=2R_1\frac{1}{6}\frac{\partial^4 U}{\partial \Delta^4}\bigg|_{\Delta=\Delta_e} \tag{7}$$

and U is expressed in terms of the interlayer spacing Δ as in Ref. [29],

$$U(\Delta)=K_{\mathrm{IL}}\left[\left(\frac{\Delta_0}{\Delta}\right)^4-0.4\left(\frac{\Delta_0}{\Delta}\right)^{10}\right] \tag{8}$$

where K_{IL} is calculated as 0.408 910 1874 J/m^2, and $\Delta_0=0.34$ nm and the equilibrium interfacial spacing is $\Delta_e=\Delta_0$. In the following analysis, both the linear and nonlinear parts of the vdW forces will be incorporated, which will induce the nonlinear vibration of the DWCNT.

2.1. Euler–Bernoulli beam model

Using the Euler–Bernoulli beam theory, the nonlinear free vibration of an embedded DWCNT under a compressive axial load can be described by the following coupled nonlinear differential equations:

$$EI_1\frac{\partial^4 w_1}{\partial x^4}+F_1\frac{\partial^2 w_1}{\partial x^2}+\rho A_1\frac{\partial^2 w_1}{\partial t^2}+p_{\mathrm{IL}}=0 \tag{9a}$$

$$EI_2\frac{\partial^4 w_2}{\partial x^4}+\frac{\partial^2 w_2}{\partial x^2}+\rho A_2\frac{\partial^2 w_2}{\partial t^2}-p_{\mathrm{IL}}-p_{\mathrm{IF}}=0 \tag{9b}$$

in which E and ρ are the Young's modulus and mass density of the CNT, $F_i(i=1,2)$ is the axial load applied on each individual tube, and I and A are second moment of inertia and cross-sectional area for the hollow cylinder. The indices 1 and 2 refer to the inner and outer tube, respectively.

If these two nested tubes are assumed to have the same end boundary conditions, they have the same vibrational modes [17]. With the consideration of the first-order vibration mode $y_1(x)$ only, the solution of Eq. (9) can thus be expressed as $w_i(x,t)=a_iy_1(x)\sin\omega t(i=1,2)$ with a_1 and a_2 representing the deflection amplitude of the inner and outer tube, respectively. Substituting this solution into Eq. (9) results in

$$EI_1a_1y_1''''(x)+F_1a_1y_1''(x)-\rho A_1\omega^2a_1y_1(x)-c_1(a_2-a_1)y_1(x)$$

$$-c_3(a_2-a_1)^3y_1^3\sin^2\omega t=0 \tag{10a}$$

$$EI_2a_2y_1'''(x)+F_2a_2y_1''(x)-\rho A_2\omega^2a_2y_1(x)+c_1(a_2-a_1)y_1(x)+c_3(a_2-a_1)^3y_1^3\sin^2\omega t+\alpha_1a_2y_1(x)+\alpha_3a_2^3y_1^3\sin^2\omega t=0 \tag{10b}$$

where a prime denotes the derivative with respect to x. The governing equations for the linear vibration of the embedded DWCNT can be obtained simply by letting $c_3=\alpha_3=0$ in Eq. (10). Assuming $y_1(x)=\exp(\lambda_1 x)$ in which λ_1 is the first eigenvalue of the characteristic equation for the linear vibration, two resonant frequencies corresponding to the first-order vibration mode can be determined provided the end conditions of the CNT are given. However, for such a nonlinear vibration, the deflection amplitude is frequency-dependent and can be determined with approximate analytical solutions. Following the same procedure of applying harmonic balance method [20,21,26,31], Eq. (10) becomes

$$\gamma_1a_1+F_1\beta a_1-\omega^2\eta_1a_1-n_1(a_2-a_1)-n_3(a_2-a_1)^3=0 \tag{11a}$$

$$\gamma_2a_2+F_2\beta a_2-\omega^2\eta_2a_2+n_1(a_2-a_1)+n_3(a_2-a_1)^3+m_1a_2+m_3a_2^3=0 \tag{11b}$$

in which

$$\gamma_i=EI_i\lambda_1^4\int_0^L[y_1(x)]^2\times\int_0^{2\pi/\omega}\sin^2\omega t dt,\quad (i=1,2)$$
$$\eta_i=\rho A_i\int_0^L[y_1(x)]^2\times\int_0^{2\pi/\omega}\sin^2\omega t dt,\quad (i=1,2)$$
$$\beta=\lambda_1^2\int_0^L[y_1(x)]^2\times\int_0^{2\pi/\omega}\sin^2\omega t dt$$
$$m_1=\alpha_1\int_0^L[y_1(x)]^2\times\int_0^{2\pi/\omega}\sin^2\omega t dt$$
$$m_3=\alpha_3\int_0^L[y_1(x)]^4\times\int_0^{2\pi/\omega}\sin^4\omega t dt$$
$$n_1=c_1\int_0^L[y_1(x)]^2\times\int_0^{2\pi/\omega}\sin^2\omega t dt$$
$$n_3=c_3\int_0^L[y_1(x)]^4\times\int_0^{2\pi/\omega}\sin^4\omega t dt \tag{12}$$

Thus, the relation between the deflection amplitude and the resonant frequency can be obtained from Eq. (11). If the surrounding medium effect and the axial load are ignored, i.e. $F_1=F_2=m_1=m_3=0$, Eq. (11) is reduced to the same equation derived in Ref. [21]. Without considering the axial load effect, for the case of a linear vibration of the embedded DWCNT (both vdW interactions between two adjacent tubes and between the outer surface of the CNT and the surrounding medium are assumed as linear, i.e., $c_3=0$ and $\alpha_3=0$), the resonant frequencies ω_{LE} corresponding to the first-order mode are determined by the following equations:

$$\det\begin{bmatrix} EI_1\lambda_1^4-\rho A_1\omega_{LE}^2+c_1 & -c_1 \\ -c_1 & EI_2\lambda_1^4-\rho A_2\omega_{LE}^2+c_1+\alpha_1\end{bmatrix}=0 \tag{13}$$

which gives the same formula developed by Yoon et al. [17] and Amin et al. [19]. It is obvious from Eq. (13) that there are two resonant frequencies, the lower and the upper resonant frequencies, for each vibration mode number.

2.2. Timoshenko beam model

Double Timoshenko beam model is also adopted in the current work in order to consider the effects of shear deformation and rotary inertia. Using this beam theory, the vibration of the embedded DWCNT under a compressive axial force and the nonlinear interlayer and interfacial vdW forces is described by

$$KA_1G\left(\frac{\partial^2w_1}{\partial x^2}-\frac{\partial\psi_1}{\partial x}\right)-F_1\frac{\partial\psi_1}{\partial x}-p_{IL}-\rho A_1\frac{\partial^2w_1}{\partial t^2}=0 \tag{14a}$$

$$EI_1\frac{\partial^2\psi_1}{\partial x^2}+(F_1+KA_1G)\left(\frac{\partial w_1}{\partial x}-\psi_1\right)-\rho I_1\frac{\partial^2\psi_1}{\partial t^2}=0 \tag{14b}$$

$$KA_2G\left(\frac{\partial^2w_2}{\partial x^2}-\frac{\partial\psi_2}{\partial x}\right)-F_2\frac{\partial\psi_2}{\partial x}+p_{IL}+p_{IF}-\rho A_2\frac{\partial^2w_2}{\partial t^2}=0 \tag{15a}$$

$$EI_2\frac{\partial^2\psi_2}{\partial x^2}+(F_2+KA_2G)\left(\frac{\partial w_2}{\partial x}-\psi_2\right)-\rho I_2\frac{\partial^2\psi_2}{\partial t^2}=0 \tag{15b}$$

where $\psi_i(i=1,2)$ is the rotation angle of the cross section of each individual tube due to bending and $G=0.5(E/(1+\upsilon))$ is shear modulus with υ being the Poisson's ratio. For each CNT layer treated as a single beam with hollow annular cross section, the shear correction factor K is given as $K=2((1+\upsilon)/(4+3\upsilon))$ [32]. The harmonic solutions of a double Timoshenko beam for the first-order mode can be expressed as

$$w_i(x,t)=a_iy_1(x)\sin\omega t \tag{16a}$$

$$\psi_i(x,t)=b_i\Psi_1(x)\sin\omega t \tag{16b}$$

where $i=1,2$ represents the inner and outer tube, respectively. Substituting Eq. (16) into Eqs. (14) and (15) and making lengthy manipulation results in the following governing equations:

$$\begin{aligned}&EI_1[s_1y_1'''a_1+c_1y_1''(a_2-a_1)+3c_3(y_1^2y_1''+2y_1y_1'^2)(a_2-a_1)^3\sin^2\omega t\\&+\rho A_1\omega^2y_1''a_1]+(F_1+s_1)[F_1y_1''a_1-c_1y_1(a_2-a_1)\\&-c_3y_1^3(a_2-a_1)^3\sin^2\omega t-\rho A_1\omega^2y_1a_1]\\&+\rho I_1\omega^2[s_1y_1''a_1+c_1y_1(a_2-a_1)+c_3y_1^3(a_2-a_1)^3\sin^2\omega t\\&+\rho A_1\omega^2y_1a_1]=0\end{aligned} \tag{17}$$

$$\begin{aligned}&EI_2\{s_2y_1'''a_2-c_1y_1''(a_2-a_1)-3(y_1^2y_1''+2y_1y_1'^2)[c_3(a_2-a_1)^3\\&+\alpha_3a_2^3]\sin^2\omega t-\alpha_1y_1''a_2+\rho A_2\omega^2y_1''a_2\}+(F_2+s_2)\{F_2y_1''a_2\\&+c_1y_1(a_2-a_1)+y_1^3[c_3(a_2-a_1)^3+\alpha_3a_2^3]\sin^2\omega t\\&+\alpha_1y_1a_2-\rho A_2\omega^2y_1a_2\}+\rho I_2\omega^2[s_2y_1''a_2-c_1y_1(a_2-a_1)\\&-y_1^3[c_3(a_2-a_1)^3+\alpha_3a_2^3]\sin^2\omega t-\alpha_1y_1a_2+\rho A_2\omega^2y_1a_2]=0\end{aligned} \tag{18}$$

in which $s_1=KA_1G$ and $s_2=KA_2G$. Similarly, by applying the harmonic balance method, the relationship between the amplitudes a_1, a_2 and the resonant frequency ω of the first vibration mode can be obtained from the following two equations:

$$T_{11}\omega^4+T_{12}\omega^2+T_{13}=0 \tag{19a}$$

$$T_{21}\omega^4+T_{22}\omega^2+T_{23}=0 \tag{19b}$$

in which

$$\begin{aligned}T_{11}&=\rho I_1\eta_1a_1\\T_{12}&=\rho I_1[s_1\beta a_1+n_1(a_2-a_1)+n_3(a_2-a_1)^3]+(EI_1\lambda_1^2-F_1-s_1)\eta_1a_1\\T_{13}&=s_1\gamma_1a_1+EI_1\lambda_1^2[n_1(a_2-a_1)+9n_3(a_2-a_1)^3]\\&\quad+(F_1+s_1)[F_1\beta a_1-n_1(a_2-a_1)-n_3(a_2-a_1)^3]\\T_{21}&=\rho I_2\eta_2a_2\\T_{22}&=\rho I_2[s_2\beta a_2-n_1(a_2-a_1)-n_3(a_2-a_1)^3-m_1a_2\\&\quad-m_3a_2^3]+(EI_2\lambda_1^2-F_2-s_2)\eta_2a_2\\T_{23}&=s_2\gamma_2a_2+EI_2\lambda_1^2[-n_1(a_2-a_1)-9n_3(a_2-a_1)^3-m_1a_2-9m_3a_2^3]\\&\quad+(F_2+s_2)[F_2\beta a_2+n_1(a_2-a_1)+n_3(a_2-a_1)^3+m_1a_2+m_3a_2^3]\end{aligned} \tag{20}$$

It should be noted that the linear resonant frequencies of the embedded DWCNT calculated by the Timoshenko beam theory can be reduced to the results obtained in Ref. [19] by letting

$F_1=F_2=c_3=\alpha_3=0$ in Eq. (19). It is anticipated that Eq. (19) gives as many as four different resonant frequencies for the first-order mode vibration.

3. Numerical results and discussions

In order to investigate the effects of the polymer matrix interfacial vdW forces (α_1 and α_3) and the interlayer vdW forces (c_1 and c_3) on the vibrational behavior of the embedded CNT, the relationship between the deflection amplitude and the resonant frequency of the embedded DWCNT with simply support (S–S) end boundary condition will be presented. In case study, it is assumed that the Young's modulus, Poisson's ratio, effective tube thickness and mass density for the embedded CNT are $E=1$ TPa, $t=0.35$ nm, $\upsilon=0.34$ and $\rho=2.3$ gcm^{-3}, respectively [17–20], and the surrounding medium of the CNT is polyethylene. For a beam with S–S end boundary condition, the first vibration mode is $y_1(x)=\sin\lambda_1 x$ with $\lambda_1=(\pi/L)$. Accordingly, the deflection-dependent resonant frequencies can be determined using the Euler–Bernoulli and Timoshenko beam models from Eqs. (11) and (19), respectively.

Without considering the axial load effect Fig. 1 shows the deflection amplitude of vibration versus the resonant frequency ω for an embedded DWCNT based on the Euler–Bernoulli beam model. The inner and outer diameters of the DWCNT are $d_1=0.7$ nm and $d_2=1.4$ nm, and the length is $L=20d_2$. The lower resonant frequency corresponds to a uni-directional vibration as shown in Fig. 1(a), in which the deflections of both tubes have the same direction, the higher resonant frequency corresponds to a bi-directional vibration as shown in Fig. 1(b), in which the deflection of the tubes are in the opposite direction. These two vibration modes for the embedded DWCNT are all noncoaxial. If the DWCNT is modeled as a single beam for simplicity [20], it will vibrate coaxially ($w_1=w_2$). As a consequence, p_{IL} becomes zero. Under such situation without considering any vdW interactions, there only exists one vibration mode as shown in Fig. 1(a) and the bi-directional mode is missed. The discrepancy observed between the curve ($p_{IL}=0$) and the others indicates the importance of considering p_{IL} in our work to model each tube as a single beam with intertube interactions. Compared with the results for the vibration of a free DWCNT ($p_{IF}=0$), it is found that the effect of the surrounding polymer medium on the resonant frequency is very significant for the uni-directional vibration. For example, the linear resonant frequencies corresponding to the linear vdW interactions are determined as 0.1171 and 2.5625 THz for the free and the embedded DWCNT, respectively. However, the surrounding medium has less effect on the bi-directional vibration of the DWCNT. The linear resonant frequencies for the free and the embedded DWCNT are very close, i.e., 7.0659 and 7.3491 THz, respectively.

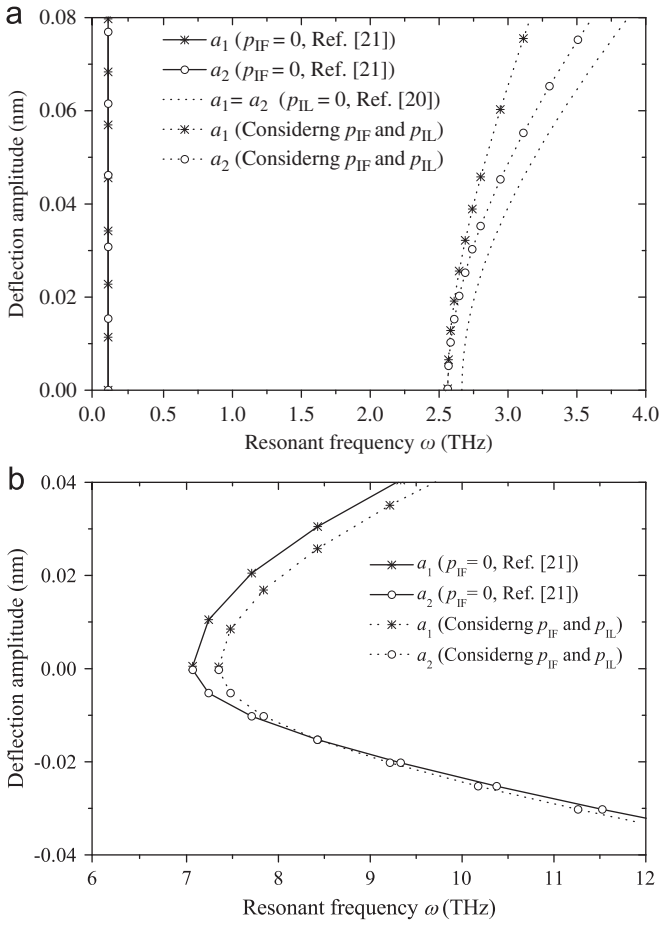

Fig. 1. Effect of interfacial and interlayer vdW forces p_{IF} and p_{IL} on the nonlinear vibrational mode of a DWCNT with S–S end boundary condition ($d_2=1.4$ nm and $L=20d_2$) (a) uni-directional mode and (b) bi-directional mode.

For the uni-directional vibration, it is found in Fig. 1(a) that the resonant frequency for the free DWCNT is almost invariable when the deflection amplitude increases from 0 to 0.08 nm. In addition, the deflection amplitude ratio of the inner tube to the outer tube is approximately 1.0003, which means a coaxial vibration. On the other hand, the dependence of the resonant frequency on the deflection amplitude for the embedded CNT is more sensitive, especially for the outer tube. It should also be noted that the deflection amplitude ratio of the inner tube to outer tube for the embedded DWCNT keeps changing with the resonant frequency and does not equal to 1, which indicates a noncoaxial vibration. However, for the bi-directional mode, both the free DWCNT and the embedded DWCNT experience noncoaxial vibration.

In order to reveal the CNT size effect on the nonlinear resonant frequencies and the deflection amplitudes of the embedded DWCNT, the deflection amplitude-frequency curves of the embedded DWCNTs with different diameters for both uni-directional and bi-directional vibration modes are depicted in Fig. 2 for comparison based on the Euler–Bernoulli beam model. The length-to-diameter ratio is kept constant as $(L/d_2)=20$ and $d_1=d_2-2t$. It is found in Fig. 2(a) that the deflection amplitude at a given resonant frequency for the uni-directional vibration increases with the tube diameter, which has the similar trend as an embedded SWCNT observed in Ref. [20]. However, the CNT diameter effect on the bi-directional vibration of the embedded DWCNT is different. For a given resonant frequency, the deflection amplitude of the inner tube decreases with the increasing of the CNT tube diameter, while the deflection amplitude of the outer tube layer becomes more complicated. It decreases with the increasing of the CNT diameter as long as the resonant frequency is smaller than a specific value, while this situation is completely reversed once the frequency is bigger than this value. For both uni-directional and bi-directional vibrations, when the diameter is large enough, for example, $d_2=3.5$ nm in the current case, the CNT size effect on the resonant frequencies is not significant, while these results are not shown in these figures. Fig. 3 shows the CNT length effect on the nonlinear resonant frequencies of the embedded DWCNT for both uni-directional and bi-directional mode vibrations. The inner and outer diameters of the CNT are kept constant as $d_1=0.7$ nm and $d_2=1.4$ nm. It is indicated in this figure that the resonant frequencies of the embedded DWCNT decrease with the increasing of the CNT length for both of these two modes. However, when the CNT length-to-diameter ratio is relatively big, for example, $(L/d_2)>30$, the CNT length effect upon

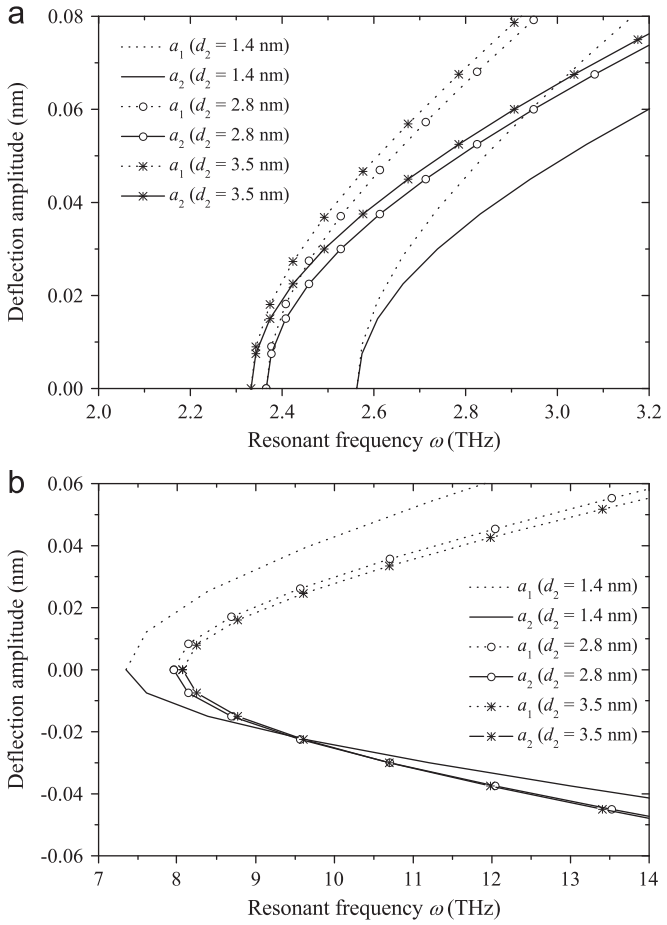

Fig. 2. CNT size effect on the nonlinear resonant frequencies of an embedded DWCNT with S–S end boundary condition ($L=20d_2$ and $d_1=d_2-2t$) (a) uni-directional mode and (b) bi-directional mode.

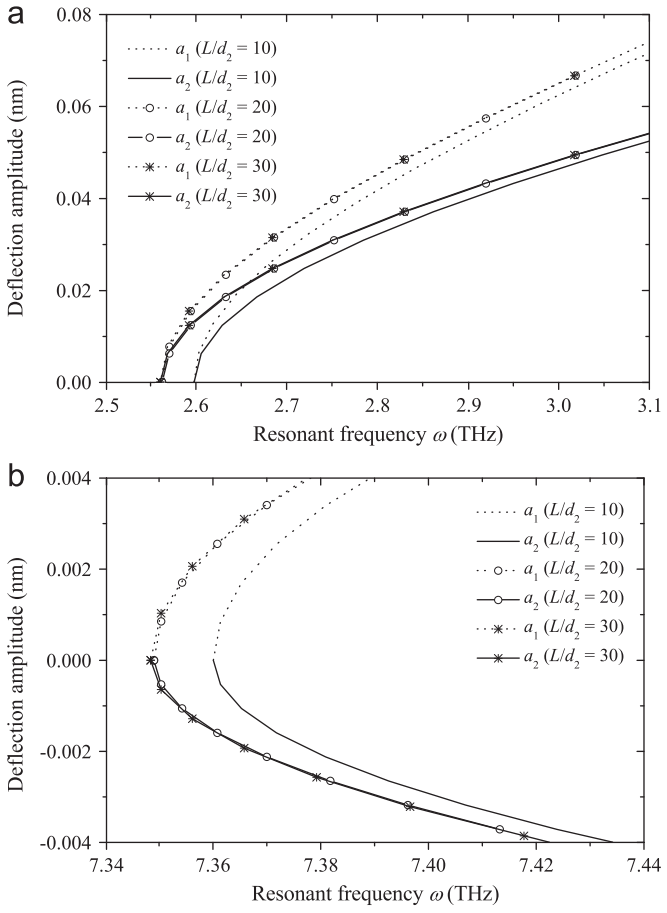

Fig. 3. Effect of CNT length-to-diameter ratio on the nonlinear resonant frequencies of an embedded DWCNT with S–S end boundary condition ($d_1=0.7$ nm and $d_2=1.4$ nm) (a) uni-directional mode and (b) bi-directional mode.

the resonant is not obvious. It is found in Figs. 2 and 3 that the CNT size effect on the deflection amplitude-resonant frequency relation of the embedded DWCNT has the similar trend as that for the embedded SWCNT in Ref. [20].

Fig. 4 demonstrates the effect of the axial load on the vibrational behavior of the embedded DWCNT with $d_1=0.7$ nm, $d_2=1.4$ nm and length $L=20d_2$ predicted by the Euler–Bernoulli beam model. The axial load is applied as a compressive strain ε. Since this applied compressive load softens the CNT; the resonant frequency of the embedded DWCNT for both uni-directional and bi-directional modes decreases with the increasing of the axial compressive strain, as expected. This axial load effect on the uni-directional vibration is more significant. Particularly, the linear resonant frequencies corresponding to $\varepsilon=0$, 0.05 and 0.1 are 2.5625, 2.5086 and 2.4534 THz for the uni-directional mode and 7.3491, 7.3304 and 7.3117 THz for the bi-directional mode, respectively.

There is an expectation that Timoshenko beam model, which takes into account shear deformation and rotary inertia effects, may provide more accurate prediction for the vibrational behavior of a CNT with smaller length-to-diameter ratio. Table 1 lists the linear resonant frequencies of both free and embedded DWCNT predicted by the Euler–Bernoulli and Timoshenko beam models. Since Timoshenko beam theory is capable of capturing both bending and shear deformation modes [33], the present double Timoshenko beam model for the embedded DWCNT is expected to give as many as four different resonant frequencies for a given mode number. It is found in Table 1 that the first two resonant frequencies of the Timoshenko beam model are close but smaller than those predicted by the Euler–Bernoulli beam theory, which overestimates the resonant frequencies for a linear vibration. It is noted that the difference between the values of the resonant frequencies predicted by different beam models in this study is larger for a free DWCNT in comparison with an embedded DWCNT. In other words, the Euler–Bernoulli beam model may provide as accurate prediction on the first-order mode vibration for an embedded CNT as the Timoshenko beam model even for the beams with smaller length-to-diameter ratios. This is due to the medium effect and agrees well with the observations in the existing studies [19,20].

It is also found in this table that the first resonant frequency of the free DWCNT is corresponding to the coaxial vibration with $a_1/a_2\approx 1$, while the others correspond to the noncoaxial vibration. Due to the constraint from the surrounding polymer medium, the vibration of the embedded DWCNT is always noncoaxial. The lowest resonant frequency corresponds to the uni-directional vibration, while the upper resonant frequencies are related to the bi-directional vibration. To clarify this Fig. 5 shows four different modes of nonlinear vibration related to the first-order mode number ($n=1$) for the free and the embedded DWCNT with $d_2=1.4$ nm and $L=10d_2$. The insets in this figure are used to magnify the first and third modes. As can be seen in this figure, the first and second modes, which can also be predicted by the Euler–Bernoulli beam model exhibit a hardening nonlinearity, i.e., the deflection amplitude increases with the resonance frequencies. However, the third and forth modes exhibit a softening nonlinearity in which the deflection amplitude decreases with the

resonant frequencies. This softening behavior can only be captured by the Timoshenko beam theory, which is reported for the first time in this work. It is obvious from Table 1 and Fig. 5 that the deflection of the inner and outer tubes differs more prominent for the third and forth modes in comparison to the first and second modes. Comparing the results of the free DWCNT in Fig. 5(a) with the embedded one in Fig. 5(b), it can be concluded that the surrounding medium has a very significant effect on the relation between the resonant frequency and the deflection amplitude for the uni-directional vibration in comparison to the other bi-directional vibration modes. For example, the value of the linear resonant frequency for the uni-directional vibration mode increases from 0.4529 to 2.5859 THz and the amplitude ratio changes from 1.0037 to 1.2487, and a coaxial vibration changes to a noncoaxial vibration.

Up to now, all the analysis is related to the first-order vibration mode $y_1(x)$ only. To further investigate the applicability of each beam model for CNTs with smaller length-to-diameter ratio and the effect of surrounding medium for higher vibration mode, the linear resonant frequencies for the transverse vibration of a free and an embedded DWCNT for different mode numbers n are calculated by both the Euler–Bernoulli and Timoshenko beam models and are listed in Table 2. The DWCNT has inner and outer

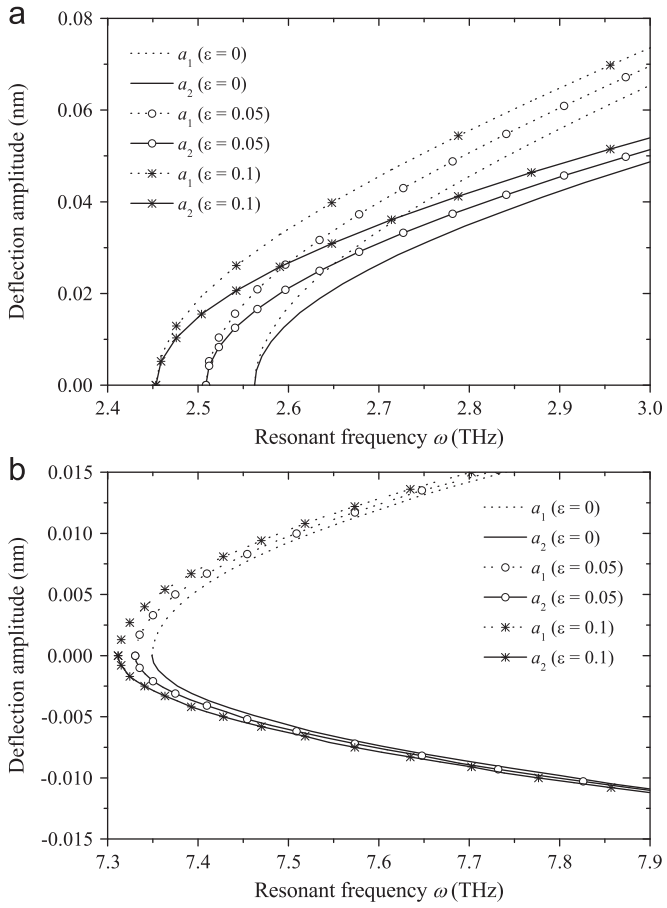

Fig. 4. Effect of axial load on the nonlinear resonant frequencies of an embedded DWCNT with S–S end boundary condition (d_1=0.7 nm, d_2=1.4 nm and L=20d_2) (a) uni-directional mode and (b) bi-directional mode.

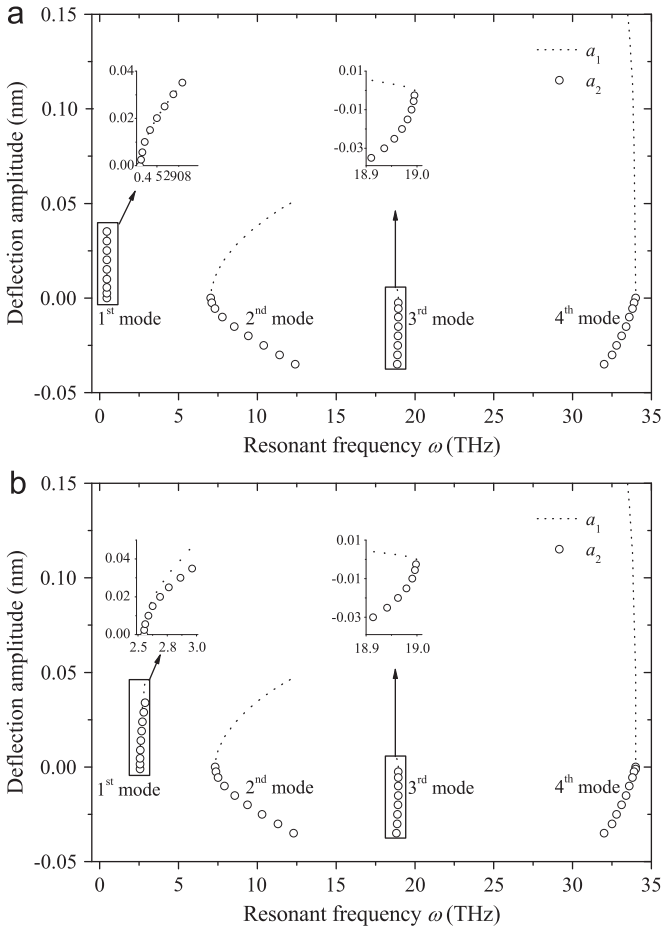

Fig. 5. Nonlinear vibrational modes of a DWCNT related to the first-order mode number (n=1) predicted by the Timoshenko beam model (d_1=0.7 nm, d_2=1.4 nm and L=10d_2) (a) free DWCNT and (b) embedded DWCNT.

Table 1
The first-order (n=1) resonant frequencies of a free and an embedded DWCNT with S–S end boundary condition predicted by Euler–Bernoulli and Timoshenko beam models (d_1=0.7 nm and d_2=1.4 nm).

	L/d_2		Uni-directional mode		Bi-directional mode			
			Euler	Timoshenko	Euler	Timoshenko		
Free DWCNT	10	ω (THz)	0.4683[a]	0.4529	7.0760[a]	7.0506	18.9453	34.0226
		a_1/a_2	1.0041[a]	1.0037	−1.9919[a]	−2.0116	−0.1016	−68.1970
	20	ω (THz)	0.1171[a]	0.1161	7.0659[a]	7.0591	18.4207	33.7317
		a_1/a_2	1.0003[a]	1.0002	−1.9995[a]	−2.0049	−0.1086	−67.2904
Embedded DWCNT	10	ω (THz)	2.5986	2.5859	7.3601	7.3298	18.9490	34.0226
		a_1/a_2	1.2506	1.2487	−1.5992	−1.6175	−0.1016	−67.5578
	20	ω (THz)	2.5625	2.5596	7.3491	7.3409	18.4218	33.7317
		a_1/a_2	1.2456	1.2452	−1.6057	−1.6107	−0.1086	−66.6512

[a] These values are calculated by the model in Ref. [21] using the parameters in Eq. (6) of the current work.

Table 2
The resonant frequencies of a free and an embedded DWCNT with S–S end boundary condition predicted by Euler–Bernoulli and Timoshenko beam models for different mode numbers ($d_1=0.7$ nm, $d_2=1.4$ nm and $L=10d_2$).

Mode number n	Uni-directional resonant frequency ω (THz)				Bi-directional resonant frequency ω (THz)			
	Free		Embedded		Free		Embedded	
	Euler	Timoshenko	Euler	Timoshenko	Euler	Timoshenko	Euler	Timoshenko
1	0.4683	0.4529	2.5986	2.5859	7.0760	7.0506	7.3601	7.3298
2	1.8611	1.6565	3.1106	2.9839	7.2385	7.1321	7.5378	7.4134
3	4.0581	3.3008	4.6063	4.0405	7.9706	7.5450	8.3317	7.8480
4	6.5654	5.1369	6.7052	5.5380	10.0944	8.4448	10.5199	8.7787
5	9.0116	7.0381	9.0335	7.2509	14.1713	9.8264	14.5281	10.1773

diameters of $d_1=0.7$ nm and $d_2=1.4$ nm, and length of $L=10d_2$. For simply supported DWCNT, its vibration modes are $y_n(x)=\sin\lambda_n x$ with $\lambda_n=n\pi/L$ $(n=1,2\ldots)$. It is observed in Table 2, as the mode number n increases from 1 to 5, the difference between uni-directional resonant frequencies obtained by the Euler–Bernoulli and Timoshenko bream models increases. For example, the discrepancy is calculated to increase from 3.4% to 28% for the free DWCNT and from 0.5% to 24.6% for the embedded one. A similar trend on the discrepancy between the Euler–Bernoulli and the Timoshenko predictions is also observed for the bi-directional vibration. From the current analysis, it is concluded that the applicability of different beam models highly depends on the vibration mode numbers when they are applied to predict the vibrational behavior of CNTs. Timoshenko beam model is highly recommended for the higher-mode vibration analysis of CNTs, for which the effects of shear deformation and rotary inertia cannot be neglected.

4. Conclusion

In summary, the nonlinear free vibrational behavior of a double-walled carbon nanotube (DWCNT) embedded in a polymer matrix subjected to a compressive axial load has been studied with the consideration of the nonlinear interlayer van der Waals (vdW) forces between two adjacent tubes and the nonlinear interfacial vdW forces from the surrounding medium. Both the Euler–Bernoulli and Timoshenko beam models are applied to derive the deflection dependent resonant frequencies. The results show that the surrounding medium has a significant effect on the vibrational behavior of the embedded CNT, which are quite different from that of the free CNT. Due to the surrounding medium effect, all the vibration modes of the embedded DWCNT are noncoaxial. It is also found that the surrounding medium effect on the uni-directional vibration is more pronounced than the bi-directional vibration.

A softening behavior on the deflection amplitude-resonant frequency relation is captured by the Timoshenko beam theory, which is reported for the first time in literature. Comparing the results predicted by these two beam models, it is found that the Euler–Bernoulli beam model may provide as accurate results for the first-order mode vibration of the embedded CNT as the Timoshenko beam model even for beams with smaller length-to-diameter ratio due to the surrounding medium effect. However, the Timoshenko beam model is highly recommended for the higher-mode vibration analysis of CNTs due to the effects of shear deformation and rotary inertia. This comprehensive analysis on the vibration of MWCNTs is expected to be helpful for the design and applications of CNT-based resonators, sensors and nanocomposites.

Acknowledgement

This work is supported by the Natural Sciences and Engineering Research Council of Canada (NSERC).

References

[1] S. Iijima, Nature 354 (1991) 56.
[2] M.M.J. Treacy, T.W. Ebbesen, J.M. Gibson, Nature (London) 381 (1996) 678.
[3] B.I. Yakobson, C.J. Brabec, J. Bernholc, Phys. Rev. Lett. 76 (1996) 2511.
[4] T.W. Ebbesen, H.J. Lezec, H. Hiura, J.W. Bennett, H.F. Ghaemi, T. Thio, Nature (London) 382 (1996) 54.
[5] T.W. Tombler, C. Zhou, L. Alexseyev, J. Kong, H. Dai, L. Liu, C.S. Jayanthi, M. Tang, S.Y. Wu, Nature (London) 405 (2000) 769.
[6] M.F. Yu, B.S. Files, S. Arepalli, R.S. Ruoff, Phys. Rev. Lett. 84 (2000) 5552.
[7] P. Zhang, Y. Huang, H. Gao, K.C. Hwang, ASME J. Appl. Mech. 69 (2002) 454.
[8] P.M. Ajayan, O.Z. Zhou, Top. Appl. Phys. 80 (2001) 391.
[9] M.S. Dresselhaus, P. Avouris, Top. Appl. Phys. 80 (2001) 1.
[10] A. Bachtold, P. Hadley, T. Nakanishi, C. Dekker, Science 294 (2001) 1317.
[11] J. Hafner, C. Cheung, C. Lieber, Nature (London) 398 (1999) 761.
[12] H. Dai, Surf. Sci. 500 (2002) 218.
[13] K.T. Lau, D. Hui, Compos. Part B 33 (2002) 263.
[14] L.W. Chen, C.L. Cheung, P.D. Ashby, C.M. Lieber, Nano Lett. 4 (2004) 1725.
[15] H.R. Lusti, A.A. Gusev, Modelling Simul. Mater. Sci. Eng. 12 (2004) S107.
[16] Y.M. Fu, J.W. Hong, X.Q. Wang, J. Sound Vib. 296 (2006) 746.
[17] J. Yoon, C.Q. Ru, A. Mioduchowski, Compos. Sci. Technol. 63 (2003) 1533.
[18] M. Aydogdu, Arch. Appl. Mech. 78 (2008) 711.
[19] S.S. Amin, H. Dalir, A. Farshidianfar, Comput. Mech. 43 (2009) 515.
[20] M.H. Mahdavi, L.Y. Jiang, X. Sun, J. Appl. Phys. 106 (2009) 114309.
[21] K.Y. Xu, X.N. Guo, C.Q. Ru, J. Appl. Phys. 99 (2006) 064303.
[22] K.Y. Xu, E.C. Aifantis, Y.H. Yan, ASME J. Appl. Mech. 75 (2008) 0210131.
[23] L.L. Ke, Y. Xiang, J. Yang, S. Kitipornchai, Comput. Mat. Sci. 47 (2009) 409.
[24] C.Y. Wang, C.Q. Ru, A. Mioduchowski, J. Appl. Phys. 97 (2005) 114323.
[25] R. Li, G.A. Kardomateas, ASME J. Appl. Mech. 74 (2007) 1087.
[26] Y. Yan, L.X. Zhang, W.Q. Wang, J. Appl. Phys. 103 (2008) 113523.
[27] Y. Lanir, Y.C.B. Fung, J. Compos. Mater. 6 (1972) 387.
[28] L.Y. Jiang, Y. Huang, H. Jiang, G. Ravichandran, H. Gao, K.C. Hwang, B. Liu, J. Mech. Phys. Solids 54 (2006) 2436.
[29] W.B. Lu, J. Wu, L.Y. Jiang, Y. Huang, K.C. Hwang, B. Liu, Philos. Mag. 87 (2007) 2221.
[30] C.Q. Ru, J. Mech. Phys. Solids 49 (2001) 1265.
[31] Y.Z. Liu, L.Q. Chen, Nonlinear Vibration, High Education, Beijing, 2001 (in Chinese).
[32] G. Cowper, ASME J. Appl. Mech. 12 (1966) 335.
[33] S.S. Rao, Mechanical Vibrations, fourth ed., Pearson Prentice Hall, New Jersey, 2004.